Attitude Determination and Control System of ThinSats

Dom Huh†, Zaeem Gauher†, Aaron Martinez†, Jay Deorukhkar*
†Undergraduate in Electrical Engineering Department
*Undergraduate in Computer Engineering Department
at Volgenau School of Engineering

***Abstract*—The attitude of a spacecraft refers to its angular orientation, and its determination and control relies on sensors, processor, and actuators. This subsystem is called the ADC (Attitude Determination and Control) system. For low-orbit satellites classified as ThinSats, the ADC can be optimized through the implementation of a tested sensor array and an networked control system with reliable communication protocols and tuned controller while adhering to the weight, size, and power specifications of the ThinSat program. The performance of the ADC is often classified by its reliability, computation cost, and net power efficiency. Thus, the paper will outline, at a high level, options that could be considered to optimize this nonlinear dynamical system within the given constraints. The paper will then discuss the design of the Wing of Daedalus(WoD) ThinSat that was engineered for the Virginia Space ThinSat Program.**

***Index Terms*—Control System Analysis, Nonlinear dynamical systems**

I. Introduction

Attitude refers to the orientation of a spacecraft with respects to a selected frame of reference. To regulate attitude, three functions must be in place: Guidance, Navigation, Control. The navigation, or otherwise called determination, provides the current attitude of the observed body. The guidance function determines the desired next state in terms of attitude. The control function gives the correct actuating instructions to reach the reference provided by the guidance function. The commonly used set of representation of attitude is the quaternion. Quaternions describe rotations and orientation within a 3-D space by introducing three complex numbers, and are utilized due to their computational efficiency and avoidance of numerical errors that arise in other methods of representation such as Euler angles and its potential for Gimbal lock. Quaternion kinematics can be further explored in [1].

A. Overview of ADC subsystem

For attitude navigation and control of a spacecraft, the attitude determination and control (ADC) system is integrated. The ADC system can be divided into three subgroups: sensor array, processor, and actuators. The sensor array provides raw relative and absolute measurement that provide insight on the spacecrafts angular orientation. This information is passed to the processor, where the estimator filters the data by methods of noise filtering and drift control via sensor fusion and stochastic filtering and transforms the filtered data into a dynamical state vector that can be mapped to the attitude of the spacecraft. The state vector informs the controller of the current attitude, which is used to create the actuating signal. Different control algorithms can be implemented in various phases of launch to develop the actuating signal. For instance, at orbital insertion, detumbling is required to stabilize angular velocity. A common approach is to implement the B-dot algorithm, whose objective function is to minimize the angular acceleration with actuators by countering the satellites rotation. Whereas in other stages, attitude behavior vastly differs. During the slew, phasing, and stabilization modes, due to the environmental factors such as solar winds or imperfect release, anomalies in attitude occurs. In addition, mission requirements may require specific desired positioning. Therefore, attitude determination and control in these situations is implemented by either a LQR, MPC, FLC, or PID controller. Once the actuating signal is calculated, it is sent from the processor to the actuators, which applies torque onto the rigid body. This system would loop this process, often along with a feedback, until it fulfills the specified mission requirements.

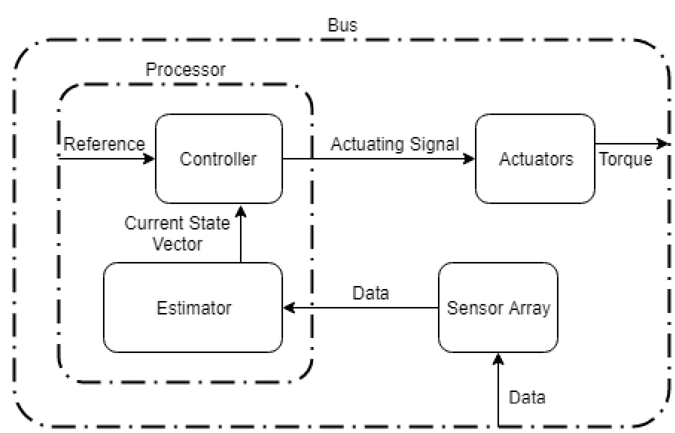

Fig. 1: Overview of ADC subsystem

B. Analysis and control of nonlinear dynamical systems

The nonlinearity property when demonstrated in a system forecasts essentially nonlinear phenomenons [2] that point to chaotic behaviors such as limit cycles, finite escape time, multiple isolated equilibria, and bifurcations. To analyze such systems for stability in cases of external perturbations, using definite functions to describe stability in terms of energy and applying Lyapunov direct method can determine existence of Lyapunov stability. Generic Lyapunov-based disturbance-rejection assessment tools have proven the asymptotic stability of attitude control systems [3]. As for the control of the system, a model predictive control approach could be implemented, however, other less complex controllers such as PID could work for simpler systems.

II. Background

A. ThinSat Specifications

The ThinSat program defines a bus design that includes power, communication, and data handling systems with an option for attitude control and determination. The weight constraint is approximately 280g, and its dimensions at 111.1 x 114.2 x 12.5 mm. The payload area is estimated to be 107 x 52 x 10 mm, with around 1.25W of power availability. [4] The deployment of the ThinSat will occur at 200-250km, with live data transmission via GlobalStar. The program aims to have ThinSats with approximately 5 days of orbit life.

B. Microcontroller

A microcontroller(MCU) can be described as a computer built upon an integrated circuit designed to run a specific function. It often consists of one or more processing cores, memory, and IO peripherals, and is seen interconnected with sensors and actuators within embedded systems.

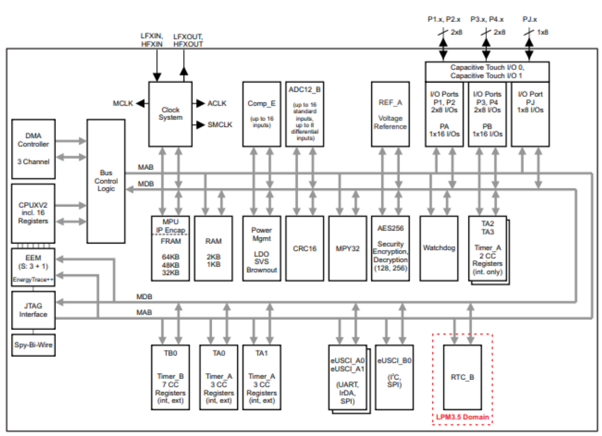

Fig. 2: Functional Block Diagram of MSP430-FR5X6X Source adapted from [5]

MSP430: The MSP430-FR5969 has a wide range of operating voltages from 3.6V to 1.8V, with various ultra-low-power modes. The architecture is a 16-bit RISC with a 16 MHZ clock, and a flexible clock system that allows for different clock frequencies. The MSP430-FR series may utilizes Ferroelectric RAM (FRAM). It is a constructed in a similar manner to DRAM but utilizes a ferromagnetic material. FRAM is less prone to single event effects in a high radiation environment. The microcontroller also has 64 KB of non-volatile memory and various analog/digital functions like an analog to digital converter (ADC). The enhanced serial communication includes UART with baud-rate detection, SPI, and I2C protocols, where UART or I2C can be used for the bootloader (BSL).

Operating System: A real time operating system (RTOS) kernel with support of the specific MCU architecture should be considered to optimize real time processes that will be used in the ADC system. Key features of RTOS include minimal queuing delay, interrupt latency, context switching latency, jitters, and a well-implemented scheduling algorithm. FreeRTOS can be considered for the MSP430, as it supports this embedded system as well as being open source. FreeRTOS provides upsides such as low overhead, dynamic tick configuration option, multithreading, semaphores, mutexes, and coroutine support. For the scheduling algorithm, while FreeRTOS does provide the option of cooperative scheduling, the preemptive scheduler option is common practice for hard RTOS.

C. Communication Specification

A critical consideration about communication selection must be included to ensure reliability within the ADC system. Good practice such as matching baud rate selection when using an asynchronous communication, and other common error handling methods should be followed.

UART: Universal Asynchronous Receiver/Transmitter refers to the physical circuit that consists of the following communication ports: transmit (TX), receive (RX), and ground (GND). The on-board computer (OBC) will connect its TX port with the MCU RX port, and the MCU will connect its TX port to the OBCs RX port. This ensures that the data transmitted from one device will be received from the other. The GND ports should be connected to each other. This is to ensure that both devices have the same ground reference to compare to when the data is received. As it is classified as an asynchronous serial communication, parity, acknowledgement signals, and cyclic redundancy check (CRC) should be taken into consideration for error handling. The UART communication, in short, will be used for data communication between the OBC and the MCU.

SPI: The Serial Peripheral Interface protocol is used to send data between the MCU and the two sun sensors as well as the inertial measurement sensor (IMU). This is a full-duplex protocol, meaning both devices can transmit/receive data at the same time. It is also a synchronous protocol, therefore the master and slaves share the masters clock signal to stay synchronized. It consists of four ports on each device, the Master-In-Slave-Out (MISO), the Master-Out-Slave-In (MOSI), the Serial Clock (SCLK), and the Slave Select (SS). The MCU will connect its MISO, MOSI, and SCLK ports to all of the slave devices MISO, MOSI, and SCLK ports. Since there are multiple slaves, there are multiple SS ports on the MCU, which are connected to the corresponding slave devices SS ports. Depending on which device the master wants to transmit/receive data from, it will select the specific slave device by using its corresponding SS port.

I2C: Inter-Integrated Circuit is a synchronous, multi-master, multi-slave, serial communication protocol for two-wire interface to connect low-speed devices. However, I2C faces many serious limitations such as half duplex data transmissions, and fragility in multi-slave layouts. This communication protocol should be avoided within the ADC system due to its unreliability.

D. Sensor Array

Inertial Measurement Sensor (IMU): Inertial measurement units are classified based on its degrees of freedom. The IMU with 9 degrees of freedom can record an objects linear acceleration, angular rate, and the surrounding magnetic field. Selection of an IMU requires an analysis of which type of serial communication will be used, what the response rate of the unit is, the package size, cost, and the number of degrees of freedom. A typical 9 DoF (degrees of freedom) IMU features the following 3-axis sensors.

a) Gyroscope: A gyroscope sensor contains small strips of metal that are free to bend when the gyroscope tilts or moves. The amount of bending is recorded in order to measure the angular velocity of an object. Thus, this sensor is able to obtain the pitch, roll, and yaw of an object with respect to a certain zero calibration point. However, it is necessary to zero the sensor frequently as it is prone to drift. Drift refers to long-term noise which leads to samples being continually further away from their true values. The standard approach of constantly zeroing the sensor is not feasible in a small satellite application because a stationary environment is required for calibration. Therefore, the method of accounting for the drift error by subtracting a known amount of drift per sample may be taken. This approach is also not perfect since drift error is not constant but it is more ideal for satellite missions.

b) Accelerometer: The accelerometer is a sensor that measures the proper acceleration of an object typically in all three axis. Proper acceleration does not refer to the acceleration due to changes in velocity but instead refers to the force experienced by a test mass inside the device. For instances, an accelerometer placed on the surface of the earth will indicate non-zero acceleration due to gravity even though the object is at rest. Therefore, in order to measure the roll and pitch of an object, further calculations are required. This sensor also demonstrates a prone for drift error and noise, therefore correction techniques are necessary.

c) Magnetometer: A magnetometer is a device that can detect and respond to the Earths magnetic field. There are two major types of magnetometer sensors: vector magnetometers and scalar magnetometers. The vector magnetometer measures the vector components of the magnetic field whereas the scalar magnetometer measure only the magnitude of the vector magnetic field. Choosing between the two types is completely dependent on the application where the sensor is being utilized. One major advantage of using a 9 DoF IMU is that the magnetometer data can be calibrated to the gyroscope data to reduce the drift error. However, if the magnetometer is used in an environment where ferromagnetic materials are in close proximity, the magnetometer data will not be accurate. The main use of the magnetometer in a small satellite application is for attitude control with the utilization of magnetorquers.

Sun Sensor: The Sun sensor can measure the orientation of the spacecraft in reference to the Sun. Its operation consists of outputting current into its four pinouts based on the location at which light hits the sensor. Common practice is to place a cover with a hole over the sensor so that the light meet the sensor at a smaller, more defined radius. Calculations to find the attitude of the spacecraft can be found in the datasheet, however more precise calculations can be done, which is seen in [6].

E. Estimators

Kalman Filter: Kalman filtering is integrated with sensor data for state estimation on dynamical systems. Due to the nonlinearity of the system, the unscented or the extended Kalman filter should be implemented. A Kalman filter operates by updating the present state estimation based on sensor measurements and its prior estimations. The extended Kalman filter tacks on linearizing the system by Jacobian prior to the state estimations. However, linearization only produces approximations, resulting lower performances and divergence in state estimation although it may be computationally efficient. The unscented Kalman filter, on the other hand, tacks on the unscented transform by calculating the posterior probability distribution, the mean and covariance, then heuristically mapping the sigma points to the distribution which is then used for the state estimation. The gain is also calculated differently in the UKFs, replacing the observation model by the sigma points. [7]

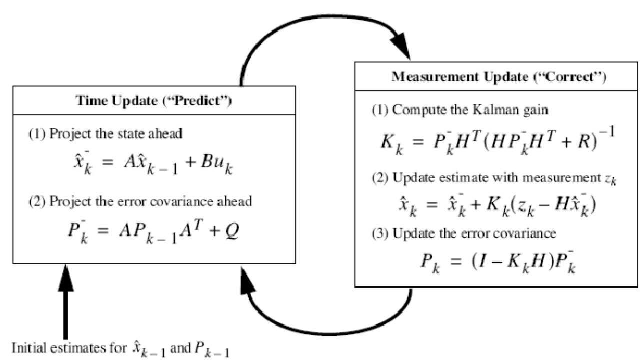

Fig. 3: Overview of Kalman Filter
Source from [8]

Particle Filter: Particle filtering can also be integrated considering its flexibility to operate on non-Gaussian distributions. However, considering the unimodality of the observation model, and the high accuracy of the sensors implemented which would result in higher sampling, the need for such a filter and the computation requirements would make PFs a worse option than an EKF or UKF. However, particle filtering based on bootstrap filtering has proven successful, and can be seen in [9].

F. Controllers

LQR: The linear-quadratic regulator algorithm is an optimal control method of tuning feedback gain within a system. Thus, it can minimize the control energy and optimize the response performance. Success in global stabilization of an nonlinear spacecraft system by a quaterion-based LQR controller can be seen in [10]. The LQR has also been proven via simulation to outperform a PD controller on cases where star trackers are used exclusively in sensor array. [11] Despite LQRs ability to better tracks a reference trajectory than PID, considering the nonlinearity and time variance properties of the attitude system and the low dimensionality of the state vector, applications of specialized LQRs are often not practical and needed.

PID: The proportional-integral-derivative controller consists of three parts: proportional, integral, and derivative. The proportional term of the PID applies a gain factor to the current error value, resulting in a proportioned response to error. The integral term of the PID takes into account past values by integrating the error over time to eliminate the steady state error. The derivative term of the PID takes into account future values by taking the derivative the error, therefore understanding the changes in the error to prevent overshooting the reference and adding in an adaptive response. This controller is lightweight, and has been prevalent in simple control systems with low dimension state vectors. Fine tuning such as heuristically adjusting the gains, clamping to avoid integral windup, filtering noise for the derivative input signal, and other methods to tune for nonlinearity is pivotal for PID controllers success.

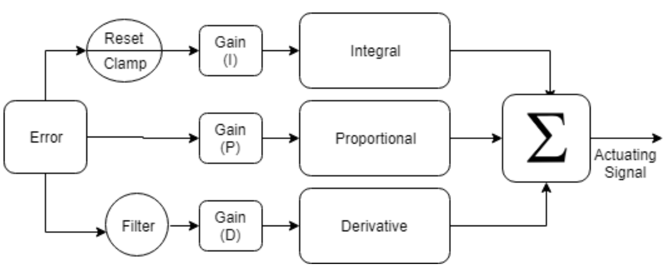

Fig. 4: Overview of PID

MPC: The model predictive control algorithm includes useful capabilities such as implementing MIMO control systems, constraint handling, and predictive actions given a foresight via sensor readings. The operation of the MCP consists of developing a model of the plant paired with an optimizer within its local scope to preview various scenarios bounded by the prediction horizon window to find the optimal actions to reach the reference. The scenario testing selection follows a systematic approach, incorporating the optimizer to minimize the difference between the reference and the prediction as well as minimizing changes in action with the constraints defined taken into consideration. When dealing with nonlinear systems, an adaptive MCP, a gain-scheduled MCP, or an nonlinear MCP must be considered. The MCP algorithm however does require higher processing power and memory storage, and therefore for a smaller system such as the ThinSat, it is not an ideal solution. There are methods to lower computation costs discussed in [12] and [13] for explicit MCP and [14] for online optimization MCP.

FLC: Fuzzy logic controller operates on a user-defined rule set based on fuzzified data, which exists within the fuzzy logic parameters. In nonlinear systems, fuzzy controllers are not ideal, as they often threshold, requiring if-then control rules, and therefore are not approximate nor adaptive. However, in simulations done by Chen, two FLC has proven more successful as they obtain a faster convergent time and lower steady-state error than two linearizing classical controller [15].

G. Actuators

Actuators are used to induce a torque on the satellite. Using actuators to apply a torque onto the satellite is a commonly used and reliable method of attitude control. There are many different implementation of actuators; however, due to construction constraints, only a few implementations were considered for the ThinSat program. The practical implementations considered for this program are momentum wheels, gravity gradient descent, and magnetic torque rods.

Momentum wheels: Momentum wheels are often used to position cameras in satellites and not intended for large movements and are considered due to their accuracy. Momentum wheels utilize the conservation of angular momentum to rotate the satellite around its center of mass to adjust the satellites attitude. This method, while precise, does have many several moving parts creating many possible points of failure.

Gravity gradient descent: Gravity gradient descent is considered due to ease of implementation. Due to the inverse square law of gravitational fields, objects in orbit will tend to align its axis of minimum moment of inertia vertically. This method is easy to implement because it only requires adjustments to the position of components. This method of attitude control will only stabilize the satellite in a fix position, this method cannot change the satellites attitude into any desired position. Additionally, gravity gradient descent requires reliable control of the satellites center of mass. Gravity gradient descent cannot be reliably implemented into this system due to the fix position of several components. While this form of attitude control will not be utilized the physical impact will have to be taken into account.

Magnetic Torquers: Magnetic Torquers are a set of three coils that are align along each current. When current is driven through the coils,th conjunction of the control algorithm. This method, while reliable and easy to construct, requires high flux density. The magnetorquers have been proven successful during detumbling by actuating the B-Dot algorithm paired with a magnetometer as seen in [16, Fig. 5].

H. Practical Design of WoD ThinSat

The architecture of the ThinSats attitude determination and control subsystem integrates a networked control system that

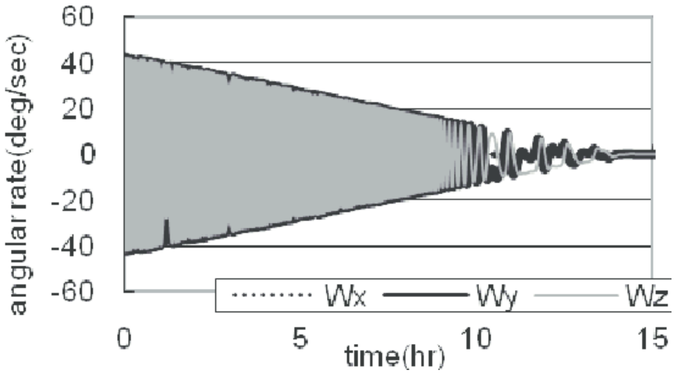

Fig. 5: Worst-case B-dot Results after Boom Extension
Source adapted from [16]

relies on different fieldbuses depending on the control chain of certain components. The UART communication will be implemented between the OBC and the MCU due to the hardware selected, while the SPI protocol will be implemented between the MPU and the sensory array. The selection of communication protocol is based on the constraints of the ThinSat architecture and the selected MCU (MSP430-FR5969) as well as reliability of SPI over I2C communication. The sensor array includes two IMU sensors with 9 degrees of freedom, as well as two sun sensors, each placed on their own respective side of the ThinSat. This layout allows for data collection throughout all possible orientations with each type of sensor in a reliable manner. The IMUs and the sun sensor will implement the UKF as their estimator, and the PID controller once detumbled. Aforementioned, detumbling will be handled by the B-dot algorithm, as it is a proven method. The actuators selected are the magnetorquers, as to fall within the weight and size constraint of the ThinSat design. Hardware in loop testing will be implemented to test the PID controller and the communication with the MSP430, magnetorquers, and the sensor array. The simulation should test if the actuating signal is sent to the correct actuators, the sensor readings are read, and the state vector is updated. Ground testing of the attitude subsystem will utilize a Helmholtz cage to test the magnetometer and the magnetorquers, providing a realistic physical testing environment.

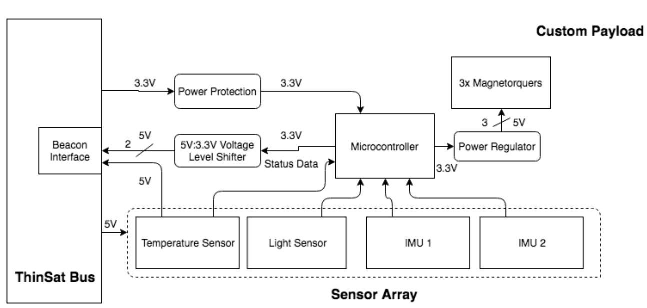

Fig. 6: Block Diagram of WoD ADC Subsystem Payload

I. *Conclusion*

Following the guidelines provided by the ThinSat program, the design of the attitude determination and control subsystem of the spacecraft considered options based on reliability, performance, and constraints. Each aspect of the ADC system was discussed, giving several possibilities within each component. Then, the paper constructed an overview of the ADC system that was considered for the launch of the WoD ThinSat in Spring 2019.

Acknowledgment

The authors would like to thank the GMU SatCom for support in research, and Snehashis Paul for technical advising.

References

[1] J. Sol, "Quaternion kinematics for the error-state Kalman filter," Arxiv, pp. 4-32, November 8, 2017[Online] Available at: https://arxiv.org/pdf/1711.02508.pdf.

[2] H. K. Khalil, "Nonlinear control.", Harlow: Pearson, 2015, pp.35-76.

[3] J. B. Aldrich, Attitude Control with Analytic Disturbance-Rejection Guarantee, Journal of Guidance, Control, and Dynamics, vol. 37, no. 6, pp. 17911807, 2014.

[4] Twiggs, R., Zucherman, A., Bujold, E., Counts, N., Colman, C., Garcia, J., Diddle, A. and Zhirkina, P. (2018). "The ThinSat Program: Flight Opportunities for Education, Research and Industry.", [online] DigitalCommons@USU. Available at: https://digitalcommons.usu.edu/smallsat/2018/all2018/475/.

[5] Texas Instruments, MSP430FR596x, MSP430FR594x Mixed-Signal Microcontrollers, MSP430FR5969 datasheet, Oct. 2012 [Revised Aug. 2018].

[6] Allgeier, Shawn Mahin, Matt Fitz-Coy, Norman. (2009). Design and Analysis of a Coarse Sun Sensor for Pico-Satellites. 10.2514/6.2009-1837.

[7] E. A. Wan and R. Van Der Merwe, "The unscented Kalman filter for nonlinear estimation," Proceedings of the IEEE 2000 Adaptive Systems for Signal Processing, Communications, and Control Symposium (Cat. No.00EX373), Lake Louise, Alberta, Canada, 2000, pp. 153-158. doi: 10.1109/ASSPCC.2000.882463.

[8] MRL Team Description 2010 - Small Size Robot League - Scientific Figure on ResearchGate. Available from: https://www.researchgate.net/figure/Kalman-filter-equations-and-instruction_fig3_283645465.

[9] Cheng, Y. and Crassidis, J. (2010). "Particle Filtering for Attitude Estimation Using a Minimal Local-Error Representation.", Journal of Guidance, Control, and Dynamics, 33(4), pp.1305-1310.

[10] Y. Yang, Analytic LQR Design for Spacecraft Control System Based on Quaternion Model, Journal of Aerospace Engineering, vol. 25, no. 3, pp. 448453, 2012.

[11] S. Beatty, Comparison of PD and LQR Methods for Spacecraft Attitude Control Using Star Trackers, 2006 World Automation Congress, 2006.

[12] Jamal Arezoo, Karim Salahshoor. "Complexity Reduction of Explicit Model Predictive Control via Combining Separator Function and Binary Search Trees.", American Journal of Computer Science and Technology. Vol. 1, No. 1, 2018, pp. 19-23. doi: 10.11648/j.ajcst.20180101.13.

[13] D. Ingole, M. Kvasnica, H. D. Silva, and J. Gustafson, Reducing Memory Footprints in Explicit Model Predictive Control using Universal Numbers, IFAC-PapersOnLine, vol. 50, no. 1, pp. 1159511600, 2017.

[14] Y. Wang and S. Boyd, Fast Model Predictive Control Using Online Optimization, IFAC Proceedings Volumes, vol. 41, no. 2, pp. 69746979, 2008.

[15] C.-H. Cheng, S.-L. Shu, and P.-J. Cheng, Attitude control of a satellite using fuzzy controllers, Expert Systems with Applications, vol. 36, no. 3, pp. 66136620, 2009.

[16] Attitude Control by Magnetic Torquer - Scientific Figure on ResearchGate. Available from: https://www.researchgate.net/figure/Worst-case-B-dot-Results-after-Boom-Extension_fig2_261711434.